

## A Comparison of Plume Rise Predictions in a Modelled and Observed Nocturnal Boundary Layer

John R. Taylor<sup>1</sup>

<sup>1</sup>School of Physical, Environmental and Mathematical Sciences  
UNSW Canberra, Canberra, ACT, 2600, Australia

### Abstract

Plume rise is a key variable in air quality modelling. The plume rise model implemented in CSIRO's The Air Pollution Model (TAPM) was implemented in MATLAB, and the plume rise through modelled and observed boundary layers compared for an overnight strongly stable period. Contrary to expectations, the plume rise height was similar in the modelled and observed boundary layers despite a large difference between the wind and temperature profiles in the two cases. In the more weakly stratified modelled boundary layer, the plume was bent over by the stronger winds and there was a much greater rate of entrainment of ambient air into the plume. This enhanced mixing limited the height of rise even though the ambient stratification was much weaker. In contrast, with the observed profiles the plume rose almost vertically, because the winds were light in the deeper nocturnal inversion, and there was a much smaller entrainment flux into the plume. Even though the plume rise height was similar in the two cases, the volume flux in the plume was much less for the observed boundary layer structure so the plume was less diluted. Based on the results of this case study, it is suggested that assessments of predicted air quality impacts need to take into account the probability that models may not adequately predict the atmospheric boundary layer structure under strongly stable conditions.

### Introduction

Typically the impact of a proposed emission on local air quality is tested by using a plume model to assess possible dispersion characteristics. However, accurate dispersion modelling requires knowledge of the vertical wind and temperature profiles in the atmospheric boundary layer, and this type of data is rarely available for a given area for the required time period. The approach generally adopted is to use an atmospheric model to generate the required profiles. The Air Pollution Model (TAPM), developed by CSIRO, has been widely used in Australia to generate the required meteorological information for environmental assessments, including several projects proposed for the Australian Capital Territory (ACT). However, [5] has shown that TAPM's performance at an ACT site was significantly worse in strongly stable conditions than in weakly stable or unstable conditions. In particular, the modelled winds were stronger than those observed and the overall static stability of the inversion layer was weaker. The discrepancy is of concern because the strongly stable conditions generally result in poor dispersion, so their occurrence and characteristics are critical for assessing air quality impacts. Over their study period, May to September 2008, [5] found a strongly stable boundary layer was present in 37% of the observations.

The first possible impact of problems in the modelled boundary layer structure would be expected to be on the height to which the emissions from a buoyant source rise. To test how the plume behaviour could vary, the predicted plume rise in a strongly stable boundary layer observed in the ACT region by [5] for the night beginning on 25 August 2008 was modelled, and compared this with the predicted plume rise in the TAPM simulated

boundary layer for the same night. To predict the plume rise, the plume model included in TAPM was implemented in MATLAB. The observations, meteorological model, and the plume rise model are discussed in the methods section. The observed and simulated boundary layers are then discussed followed by the results from the plume rise model.

### Method

#### Observations

The boundary layer observations were made at the School of Physical Environmental and Mathematical Sciences (PEMS) field site which is located in the Majura Valley, approximately 3 km northwest of Canberra International Airport (see [5] for site details). Here the focus is on a single night of observations from a longer term study which ran from the late autumn into the spring of 2008. During this observational program two ground-based remote sensing instruments were operated. For temperature profiling there was a continuous wave electromagnetic, pulsed acoustic, Radio Acoustic Sounding System (RASS) and, for wind profiling, a 5kHz Doppler sodar (or acoustic radar). Both instruments were developed and constructed within the School of PEMS. A comparison of the RASS measured temperatures with those from an ultrasonic anemometer is in [5] and with in-situ temperature measurements from a radio controlled model glider is in [6]. The RASS temperature profiles begin at 50 m Above Ground Level (AGL) and the maximum range is 620 m. Temperatures are returned at 30 m intervals. The sodar returns winds at 10 m separation between 20 m AGL and a maximum height of 290 m AGL. A comparison of the sodar measured winds and those from an ultrasonic anemometer mounted 23.3 m AGL is in [5] and with radar-tracked balloons is in [7]. For this study both RASS temperatures, and sodar winds were averaged in one hour intervals to be compatible with the output from TAPM. In addition to the remote sensing instrumentation, and ultrasonic anemometer, screen level (1.5 m AGL) temperature, relative humidity, and pressure, and winds at 2m AGL were recorded with an automatic weather station.

#### Meteorological Model

The meteorological component of TAPM is a prognostic model that solves the primitive equations in three spatial dimensions. TAPM is described in detail in [3] and model performance in [4]. The model's horizontal spatial coordinates are regular Cartesian, but a terrain following coordinate is used in the vertical direction. For the present study TAPM was configured with Canberra International Airport (149° 11.5'E, 35° 18.5'S) as the centre of a 100 by 100 point horizontal grid. Forty vertical levels were used, and at the instrument location, the lowest ten vertical grid heights set by the model were 9.3, 23.4, 46.7, 70.1, 93.5, 140.2, 187.0, 233.7, 280.5 and 327.2 m. In the horizontal, four nested grids were used with grid spacing of 10, 3, 1 and 0.4 km. The model results presented here are from the finest grid, at the grid point closest to the observation

site. The model simulation covered the period from 2400 Local Time (Local Time, LT, is Australian Eastern Standard Time, AEST=UTC+10) 30 April 2008 to 2400 LT 1 September 2008 in a single run with TAPM in non-hydrostatic mode. A detailed description of the model and comparison of the model results with the long term observations is in [5].

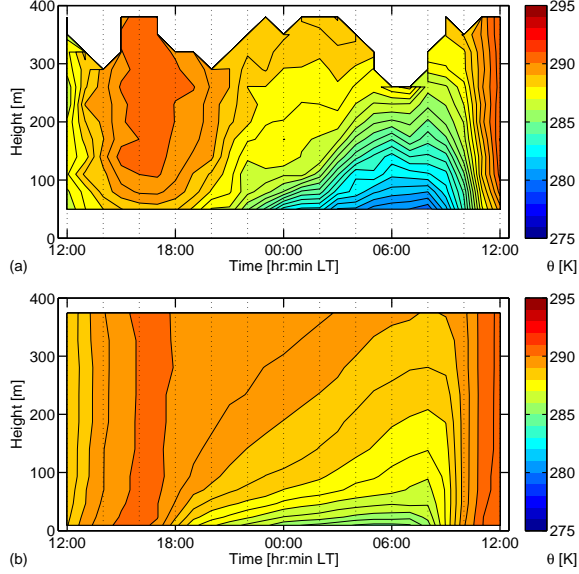


Figure 1: Time-height sections for potential temperature from (a) RASS and (b) TAPM. Color scale shows temperatures in K. Contours are at 0.5 K intervals. Both sections use hourly averaged temperature and start at 1200 LT on 25 August 2008.

### Plume Model

In an atmosphere with uniform wind and density stratification, the height of rise of a plume should depend on the initial plume buoyancy,  $F_0$ , the horizontal wind speed,  $u_a$ , and the environmental stratification, defined by the buoyancy frequency squared,  $s = \frac{g}{\theta_a} \frac{\partial \theta_a}{\partial z}$  where  $\theta_a$  is the ambient potential temperature. Dimensional arguments then give

$$z_f - z_s = 2.6 \left( \frac{F_0}{u_a s} \right)^{1/3}, \quad (1)$$

where the coefficient, 2.6, is from [1].  $z_f$  is the final height of the plume rise AGL, and  $z_s$  is the source height. It can be seen that both stronger stratification (increased  $s$ ) and greater wind speed,  $u_a$ , will reduce the height of rise of a given plume. The initial plume buoyancy flux,  $F_0$ , is defined by

$$F_0 = g w_s R_s^2 \left( 1 - \frac{T_a(z_s)}{T_s} \right), \quad (2)$$

where  $w_s$ ,  $T_s$  are the emission velocity and temperature at the source,  $T_a(z_s)$  is the ambient temperature at the source height and  $g$  is the acceleration due to gravity. Equation (1) is only applicable for an environment with constant buoyancy frequency and wind speed, both conditions not normally satisfied in the stable nocturnal boundary layer. To take into account vertical variations of these environmental parameters, [2] suggested tracking the plume by integrating the conservation equations for plume volume, vertical momentum and buoyancy fluxes with the environmental temperature,  $T_a$  and wind profiles,  $u_a = (u^2 + v^2)^{1/2}$ , are specified as functions of height. Here  $u$  and  $v$  are the west-east and south-north components of the wind vector. The plume is advected horizontally by the mean wind. A

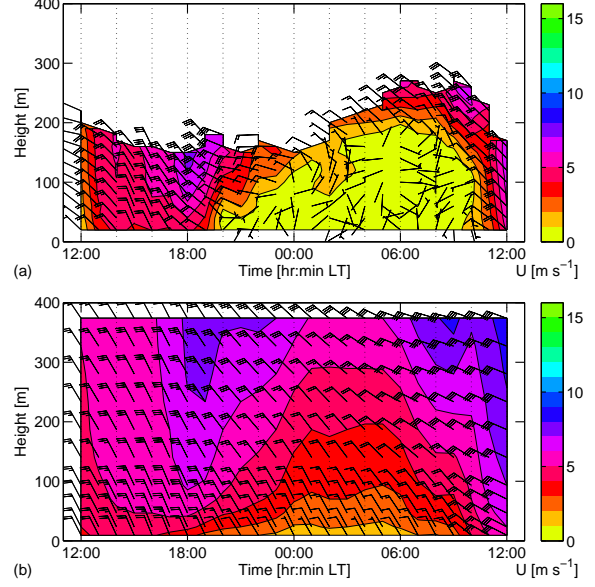


Figure 2: Time-height sections for horizontal winds from (a) the sodar and (b) TAPM. Color scale is wind speed, contours are at  $1 \text{ m s}^{-1}$  intervals. On the wind barbs, a half tail is  $1 \text{ m s}^{-1}$  and a full tail,  $2 \text{ m s}^{-1}$ . The plots show hourly averaged winds and start at 1200 LT on 25 August 2008.

similar, but slightly simplified plume model, is implemented in TAPM. The TAPM plume model is documented in [3], but for the interpretation of the present work the key equation is that for the conservation of plume volume flux,

$$\frac{dG}{dt} = 2R \left( \alpha w_p^2 + \beta u_a w_p \right), \quad (3)$$

where  $G = u_p R^2 T_a / T_p$  with  $R$  the plume radius (assuming a “top-hat” cross section), and  $u_p = (u_a^2 + w_p^2)^{1/2}$ .  $\alpha = 0.1$  and  $\beta = 0.6$  are the entrainment constants for a vertical plume and bent-over plume respectively [3]. Since mixing with the environment will rapidly reduce the plume vertical velocity from its initial value, the second term in equation 3 may dominate the growth of the plume because of the larger entrainment constant, and scaling with the ambient wind speed. The TAPM plume model was implemented in MATLAB so that the predicted plume rise in the simulated and observed boundary layers could be compared. This code was verified by comparing the plume rise predicted by the present model with that in [2] for a number of cases produced by digitising their plotted environmental temperature and wind profiles. Consistent with [3], the results from the present implementation of the TAPM plume model and the full model of [2] were in agreement.

### Results

#### Observed Versus Modelled Meteorology

Figure 1 from [5] shows time-height sections of potential temperature from the RASS and from the TAPM for the 24 hours starting from 1200 LT on 25 August 2008. Note that the colour scale and contour values are the same for both plots. The observations show greater overnight cooling than the model, although the temperature at 300 m AGL is similar. In the TAPM simulations the region of strong vertical temperature gradient is compressed into the heights below 50 to 100 m AGL. In contrast, the much greater cooling shown in the RASS observations and resulting colder near surface temperatures means that, by 0600 LT, the region of strong vertical temperature gradients extends

to over 200 m. There is also more structure within the stable boundary layer. Compare the sections between 0300 and 0600 LT. The TAPM prediction has a maximum potential temperature gradient well below 100 m, and a relatively uniform gradient above. In contrast, below 100 m the RASS profiles show the top of a high gradient region (blue contours); a weaker gradient region (blue green) above this; then another high gradient region before grading into the background temperature gradient at approximately 260 m AGL at 0600 LT. In contrast to the night time temperatures, the day time temperatures are similar in the model and RASS observations.

Figure 2, also from [5], compares time-height sections of the horizontal winds from the sodar and those from TAPM for the same time period as the potential temperature section (figure 1). Again, the colour scale and contours are the same for both plots. Although the range of the high frequency sodar is limited, the sodar and TAPM winds show a similar pattern at the upper height limit of the sodar data. For example, the sodar, just captures the wind speed maximum around 1800 LT which is clear in the model results. The most striking difference between the model results and observations is the region of very low wind speeds from 2000 LT to 1100 LT that are enclosed by the light orange-yellow colour (wind speeds of  $0.5$  to  $1 \text{ m s}^{-1}$ ) on figure 2a. The same wind speed interval only occurs at the very bottom of the TAPM section (figure 2b). The light wind area corresponds to the deep, stably stratified boundary layer visible in the RASS time-height section (figure 1a). The actual wind direction was highly variable both in height and time within the nocturnal boundary layer, but there is a clear contrast between the north westerly winds above and the variable wind direction within the light wind region. Over the same height range, TAPM shows a gradual cyclonic rotation of the wind direction moving down through the boundary layer. The wind shear is also much more uniform in the vertical in the model. In the observations, where the transition layer is visible, the shear is concentrated at the top of the almost stagnant region. The sodar derived wind vectors in the stagnant layer look noisy in figure 2a; this is partly a result of the hourly averaging as the resulting wind vectors are the residual of a complex time varying flow. Cross sections with greater time resolution show a more complex but still coherent picture of the wind speed and direction in this low wind speed region.

Stack	$z_s$ [m]	$R_s$ [m]	$w_s$ [ $\text{m s}^{-1}$ ]	$T_s$ [K]
A	35	1.50	25.0	443
B	35	1.05	29.8	773
C	56	0.52	5.9	373

Table 1: Example stack parameters from two ACT region environmental impact assessments used in the plume rise model.

#### Predicted Plume Evolution

The plume model was run for three sources that have been investigated in recent environmental impact studies for projects in the ACT. Source parameters are given in table 1. Figure 3 shows the predicted plume profiles for the three sources in the average wind and temperature profiles for the hour before 0600 LT on the 26 August 2008 and figure 4 shows the plumes' horizontal displacements. Although sources A and B had quite different exit temperatures they have very similar  $F_0$  and the predicted buoyancy fluxes fell to zero at almost the same height in both the modelled and observed atmospheres. However, both the normalised volume, and momentum, fluxes were much greater for source A than B. Source C had a smaller initial buoyancy flux and  $F = 0$  at a lower height, but this height was still similar for the observed and modelled profiles. For all three sources, al-

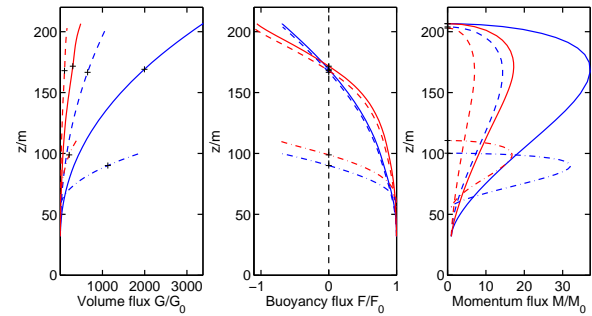


Figure 3: Predicted vertical variation of volume, buoyancy and momentum fluxes for plumes from sources A (solid line), B (dashed line), and C (dash-dot line) (table 1) in the average environmental wind and temperature profiles in the hour before 0600 LT on 26 August 2008. Blue curves for the TAPM predicted profiles and red are for the observed profiles. All fluxes are normalised by their values at the source. Crosses on volume flux (left hand panel) show  $G/G_0$  where  $F = 0$ .

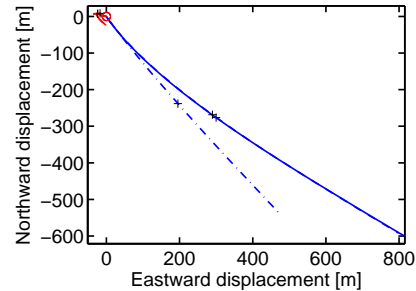


Figure 4: Predicted plume horizontal displacement from sources A, B, C (table 1) in the average profiles for the hour before 0600 LT on 25 August 2008. Colours and line types as for figure 3. Crosses show the displacements when  $F = 0$ .

though the predicted rise heights (based on the level of neutral buoyancy where  $F = 0$ ) were similar in the modelled and observed profiles, both the normalised volume fluxes,  $G/G_0$  and momentum fluxes,  $M/M_0$ , at the plume rise heights were much greater in the modelled than in the observed atmosphere. Figure 4 shows that the horizontal displacements of the plumes were much greater in the modelled atmosphere; in the observed atmosphere the plumes rose almost vertically.

The plume model was run for each hour from 1800 LT 25 August to 0900 LT the following morning. Between 1900 and 0200 LT the plume rise height was higher than the maximum height of either the sodar or RASS observations, so no solutions are available for the observed atmosphere. At the other times, the solutions the features of the plume model solutions are consistent with those at 0600 LT. The plume rise height is similar in the observed and modelled atmosphere, (figure 5a) and varies little over the night. Figure 5b shows the ratio of the heights where the plumes were neutrally buoyant,  $F = 0$ , to their maximum height where  $M = 0$  (the plumes' overshoot). The overshoot is greater for the stronger sources A and B which rise higher into the boundary layer and this trend is consistent with the weakening stratification near the top of the boundary layer.

Figure 6a, shows that for all three sources, the normalised plume volume flux,  $G/G_0$  was much greater in the observed than in the modelled boundary layer. For source C, for which solutions for all hours were available, the difference between  $G/G_0$  in the modelled and observed atmosphere increases between 2100 LT and 0200 LT, as  $G/G_0$  decreases for the predictions made using the observed profiles. This decrease occurs as the strength

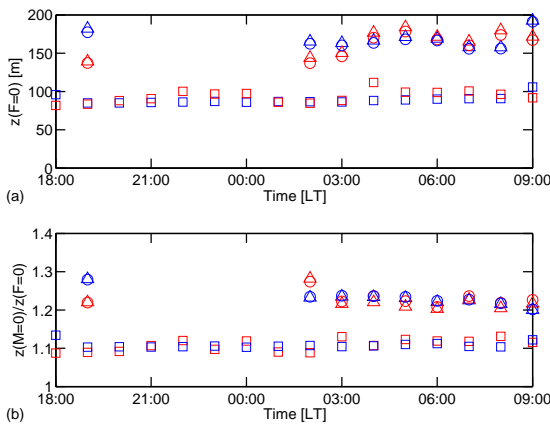


Figure 5: (a) Height (AGL) where the plume buoyancy flux first goes to zero, in the modelled (blue symbols) and observed (red symbols) boundary layers for the hours between 1800 LT 25 August 2008 and 0900 LT 26 August 2008. Sources (table 1): A, triangle, B, circle, C, square. Between 2000 LT and 0100 LT the observations did not extend to the height where  $F = 0$  for sources A and B. (b) Ratio of the height where the momentum flux,  $M = 0$ , to that where  $F = 0$ .

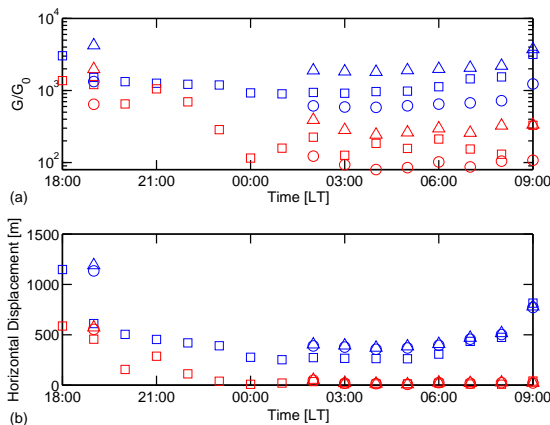


Figure 6: (a) Ratio of the volume flux in the plume to the initial volume flux,  $G/G_0$ , at the level where  $F = 0$ . (b) Predicted horizontal displacement of the plume from its source at the time that  $F = 0$ . Symbols and colours as for figure 5.

of the stratification and depth of the almost stagnant layer increases over the same time period. Also over this time interval, the horizontal displacement of the plume in the observed atmosphere decreases until the plume rises almost vertically through the atmosphere (figure 6b). The relative plume dilutions and slopes are maintained even at 0900 LT when the daytime convective boundary layer is growing rapidly in the modelled atmosphere while the observed atmosphere is still well stratified. Although the initial separation of the modelled and observed boundary layer solutions could not be followed for the two stronger sources, A and B, because of the limited height coverage of the observations, the large difference between the plume volume flux between the modelled and observed boundary layers, and the almost vertical rise of the plume, is clear in the solutions for these sources between 0200 and 0900 LT.

## Discussion

Contrary to expectations based on the difference between the observed and modelled boundary layer density stratification, the plume rise height was similar in the modelled and observed at-

mospheres. In the modelled atmosphere, the plume was bent over by the stronger winds and there was a much greater rate of entrainment of ambient air into the plume. This enhanced mixing limited the height of rise even though the ambient stratification was much weaker. In contrast in the actual profile, the plume rose almost vertically, because the winds were light in the deeper nocturnal inversion, and there was a much smaller entrainment flux into the plume. As a result, the predicted plume volume at its maximum rise height was much greater in the modelled than it was in the observed boundary layer. In addition, the stronger winds advected the emissions further from the source as the strength of the sources chosen for this case study was not sufficient for the plumes to rise through the almost stagnant part of the atmospheric boundary layer.

Under stable boundary layer conditions, major deterioration of air quality can occur when the daytime boundary layer grows to the plume rise height and the diluted emissions are mixed down to ground level. This process is called fumigation. The much reduced dilution in the rising plume than is predicted to occur with the observed atmospheric conditions means that fumigation could be a more significant problem than might be predicted on the basis of the modelled boundary layer structure. Further, for the case study, the reduced advection in the observed boundary layer would result in fumigation events potentially occurring closer to the source, and in a different direction from the source, than would be predicted based on the model meteorology.

## References

- [1] Briggs, G.A., Chimney plumes in neutral and stable surroundings, *Atmos. Env.*, **6**, 1972, 507–510.
- [2] Glendening, J.W., Businger, J.A. and Farber, R.J., Improving plume rise prediction accuracy for stable atmospheres with complex vertical structure, *J. Air Pollut. Control Assoc.*, **34**, 1984, 1128–1133.
- [3] Hurley, P., TAPM V4, part 1: technical description, *CSIRO Marine and Atmospheric Research Paper*, **25**, 2008, available from <http://www.csiro.au/Outcomes/Environment/Population-Sustainability/TAPM.aspx>, accessed 25/07/2014.
- [4] Hurley, P., TAPM V4, part 2: summary of some verification studies, *CSIRO Marine and Atmospheric Research Paper*, **26**, 2008, available from <http://www.csiro.au/Outcomes/Environment/Population-Sustainability/TAPM.aspx>, accessed 27/07/2014.
- [5] Taylor, J.R., Hirsch, A.L. and Burns, B.A., Modelling low-level boundary layer structure in complex terrain: verification of TAPM meteorological predictions in the Canberra Region, *Aust. Meteor. Oceanogr. J.*, **62**, 2012, 287–304.
- [6] Taylor, J.R., Segal, N.J., Bradshaw, M.R. and Low, D.J., 2013, Verification of RASS-measured temperature profiles using a radio-controlled model glider, *Meteor. and Atmos. Phys.*, **119**, 2013, 197–206.
- [7] Taylor, J. R., Zawa-Resa, P., Low, D. J. and Aryal, P., Verification of a mesoscale model using boundary layer wind profiler data, *Proceedings of the Australian Institute of Physics 16th Biennial Congress, Canberra, ACT, 31st January to 4th February, 2005*, available from <http://aipcongress2005.anu.edu.au/index.php?req=CongressProceedings, 2005>, accessed 25/07/2014.